Analytical Methods

Accepted Manuscript

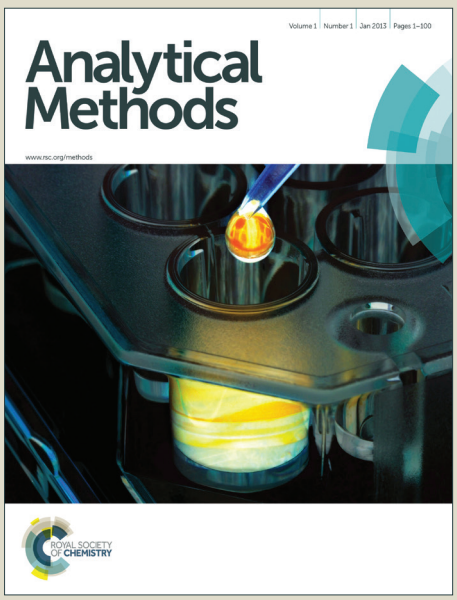

This is an *Accepted Manuscript*, which has been through the Royal Society of Chemistry peer review process and has been accepted for publication.

Accepted Manuscripts are published online shortly after acceptance, before technical editing, formatting and proof reading. Using this free service, authors can make their results available to the community, in citable form, before we publish the edited article. We will replace this *Accepted Manuscript* with the edited and formatted *Advance Article* as soon as it is available.

You can find more information about *Accepted Manuscripts* in the Information for Authors.

Please note that technical editing may introduce minor changes to the text and/or graphics, which may alter content. The journal's standard Terms & Conditions and the Ethical guidelines still apply. In no event shall the Royal Society of Chemistry be held responsible for any errors or omissions in this *Accepted Manuscript* or any consequences arising from the use of any information it contains.

ROYAL SOCIETY OF CHEMISTRY

www.rsc.org/methods

Analytical Methods

RSCPublishing

ARTICLE

Cysteine sensor based on Gold nanoparticles-Iron phthalocyanine modified graphite paste electrode

Cite this: DOI: 10.1039/x0xx00000x

Mohammed Nooredeen Abbas*[a], Ayman Ali Saeed[a], Baljit Singh[b], Abdellatef A. Radowan[a] and Eithne Dempsey[b]

Received 00th January 2012,
Accepted 00th January 2012

DOI: 10.1039/x0xx00000x

www.rsc.org/

An electrochemical sensor for the sensitive and selective detection of cysteine is proposed based on gold nanoparticles (AuNPs) – Iron(III) phthalocyanine (FePc) modified graphite paste electrode. The sensor was characterised using scanning electron microscopy (SEM/EDX), transmission electron microscopy (TEM), cyclic voltammetry and electrochemical impedance spectroscopy (EIS). Cyclic voltammetry studies demonstrated that the electrochemical behaviour of cysteine at the AuNPs–FePc modified graphite paste electrode is considerably improved compared to both the blank (unmodified) and FePc-modified graphite paste electrodes. The enhancement of the anodic redox signal for cysteine was due to a catalytic effect of gold nanoparticles which was investigated using three different graphite paste electrodes - 0.02, 0.055 and 0.11 wt% Au nanoparticles, each with a fixed quantity of FePc (5 wt%). The sensor fabricated using 0.055 wt% AuNPs resulted in optimum sensitivity as examined via differential pulse voltammetry measurements with analytical range of 50-1000 μM and a LOD of 0.27 μM. The sensor was utilised for the determination of cysteine in pharmaceutical preparations.

1. Introduction

Low-molecular mass thiols such as L-cysteine (CySH), homocysteine (Hcy) and glutathione (GSH) have been proven to play an important role in metabolism and cellular homeostasis.[1,2] The abnormal level of these biothiols is correlated with many diseases.[3] For example, L-cysteine (CySH) is one of the amino acids that play a crucial role in regulating the biological activity of protein and in the cellular antioxidant defence system.[4] CySH deficiency is involved in syndromes of slow growth in children, liver damage, and weakness. It can be synthesised in the human liver and is therefore not an essential amino acid. However, it should be supplemented in order to cover the required daily amounts. Hence, it is frequently used in food supplementary formulations and pharmaceutical preparations. Therefore, rapid and selective detection of such specific mercapto biomolecules in biological samples could help unravel complex chemical mechanisms underlying biological processes, and enhance the diagnosis and the early onset of complications. Its accurate determination in food and pharmaceutical formulations is highly demanded.

Many analytical methods, including high performance liquid chromatography[5] fluorescence microscopy[6] and chemiluminescence[7], have been proposed for the analysis of biothiols, however, they can be inconvenient and expensive.

Moreover, these methods could not satisfy the demand of analysis in complex biological systems without interference from other thiols. Due to their innate properties such as low cost, high sensitivity, fast response and size, electrochemical sensors are suited to on-site analysis.[8] Early studies indicated that bare carbon surfaces show very poor activity, even no response for L-CySH determination.[9] Bulk Au and Pt electrodes usually exhibited high overpotential due to surface oxide formation, resulting in a narrow linear range and a low selectivity.[10] However, in last decade, many electrochemical sensors based on novel nanomaterials and mediators have been designed for the detection of biothiols[11-14], improving the sensitivity and stability of those devices. Gold nanoparticles have been used to fabricate various types of modified electrodes because of their large surface area, good biocompatibility, high conductivity, renewable surface and electrocatalytic activities.

Metallophthalocyanines (MPc), the 2-dimensional 18-electron aromatic porphyrin synthetic analogues with a metal atom located at the central cavity, are of great interest due to their excellent electronic properties and potential applications in some fields such as electrical devices, solar cells and biosensors.[15-18] Currently, several research groups have explored MPc functionalized carbon nanocomposites for electrochemical biosensing applications. CoPc has been utilized either as nanoparticles modified-screen printed electrodes or as functionalized carbon nano-composites for enhanced electrocatalysis[19,20]. At the same time, CuPc and FePc in combination with carbon nanomaterials offered an excellent platform for electrochemical biosensing applications.[21-23] Herein, we have developed a new type of cysteine sensor based on the combination of the catalytic effect of AuNPs and the FePc.

2. Experimental

2.1 Materials and Methods

Graphite fine powder (<150 µm, 99.99%) and paraffin oil were purchased from Riedel-de Haën. Phthalic anhydride was purchased from Fluka. Gold(III) chloride hydrate ($HAuCl_4.xH_2O$), iron(III) chloride anhydrous (≥99.99%), L-cysteine and L-glutathione reduced were purchased from SIGMA-ALDRICH. L(+)-Ascorbic acid was purchased from BDH and DL-methionine from Reanal. Phosphate buffer solutions were prepared using 0.1 M potassium phosphate monobasic (KH_2PO_4) and 0.1 M potassium phosphate dibasic (K_2HPO_4).

2.2 Synthesis of iron(III) phthalocyanine (FePc)

Fe(III)Pc was synthesised according to the previously described method for metal phthalocyanine (MPc).[24] To a round bottom flask containing 30 mL nitrobenzene, phthalic anhydride (0.04 mole, 5.925 g), Iron(III) chloride anhydrous (0.01 mole, 1.622 g), excess of urea (25 g) and traces of ammonium molybdate tetrahydrate as a catalyst (0.01 g) were added. The reaction mixture was refluxed at 200°C with continuous stirring for approximately 5 hours, until a stable dark blue colour appearance. The solvent was excluded by filtration followed by washing with HCl (1.0 M) and NaOH (1.0 M) till a colourless filtrate obtained in each case. The synthesised iron(III) phthalocyanine catalyst is labelled as FePc onwards.

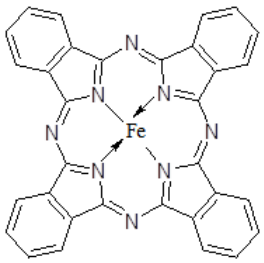

Iron phthalocyanine
Fe(III)Pc

2.3 Synthesis of gold nanoparticles (AuNPs) and AuNPs/graphite composite (AuNPs/G)

100 µL of 147mM Gold(III) chloride solution was added to 50 mL of distilled water to prepare 0.01% (w/v) solution.[25] The solution was heated until boiling. 2 mL of 1% (w/v) trisodium citrate was added rapidly under vigorous stirring. The colour changed from pale yellow to blue and finally red. The reaction solution was cooled to room temperature and stored at 4°C. The concentration of the prepared stock solution of gold nanoparticles is 58 mg/L.

This AuNPs stock solution was used to prepare the AuNPs/graphite composites with various gold nanoparticles quantities. Typically 1 g of graphite was suspended in each of 5.5 mL, 15 mL and 30 mL of AuNPs stock solution (58mg/L) in a similar fashion as that reported in literature.[26] The suspensions were heated at 100°C under moderate stirring for 5 hours in order to evaporate the water and form dried AuNPs/graphite composites (AuNPs/G) with different Au nanoparticle loadings.

2.4 Preparation of FePc modified graphite paste (FePc-GP) and FePc-AuNPs modified graphite paste (FePc-AuNPs/GP)

The FePc-GP was prepared by hand-mixing 13.5 mg of FePc catalyst in a mortar with 171 mg of graphite. Finally, 85.5 mg of paraffin oil was added and mixed well to provide paste characteristics to the mixture. FePc-AuNPs/GP was prepared in the same way i.e. FePc catalyst was mixed with the AuNPs/graphite composite followed by addition of paraffin oil and mixing. The control sample for the paste formulation was prepared by hand-mixing graphite with paraffin oil and designated as graphite paste (GP). The detailed compositions for the graphite paste (GP), FePc-graphite paste (FePc-GP) and FePc-AuNPs/graphite paste (FePc-AuNPs/GP) based electrodes are described in Table 1.

2.5 Electrode fabrication and characterisation

Scanning electron microscopy (SEM) images were captured using SEM JEOL JSM-6390LV model and transmission electron microscopy images were recorded using JEOL JEM-1230. The identity of each element was confirmed by EDX (SEM/EDX) analysis. UV-visible spectra were recorded using Shimadzu spectrophotometer (UV-2401PC). The electrochemical measurements (cyclic voltammetry, electrochemical impedance spectroscopy and differential pulse voltammetry) were performed using an electrochemical workstation CH Instruments Inc. (CHI 660D) with a platinum counter electrode and Ag/AgCl reference electrode filled with 1 M KCl. The working electrode was made from a portion of the prepared pastes (GP, FePc-GP and FePc-AuNPs/GP), and in each case the paste was filled firmly into one end of a plastic syringe (inner diameter = 0.5 cm). A copper wire was inserted through the opposite end to establish an electrical contact. Prior to use, the electrode was polished on a weighing paper to obtain a mirror-like surface.

3 Results and discussion

3.1 Surface morphological characterisation

SEM and EDX analysis together provide information regarding morphology and elemental composition of the proposed material. SEM images (Fig. 1) were recorded at different magnifications for graphite paste and AuNPs-FePc modified graphite paste samples. From the SEM images, it is difficult to predict the size and distribution of Au nanoparticles within the carbon paste, either due to the small size of the particles and/or the fact that very small amounts of AuNP (0.055%) was mixed with the graphite paste. However, from the comparison (Fig. 1(a-f)) of the graphite paste and FePc-AuNPs modified paste samples (FePc-AuNPs/GP), over different magnifications, morphology differences are evident. Elemental identification was confirmed via the energy dispersive X-ray analysis (SEM/EDX, Fig. 1g), by making measurements over the randomly chosen areas. The presence of C (due to graphite), Fe (due to FePc) and Au (due to Au nanoparticles) confirm the dispersion and composition of the modified carbon paste (FePc-AuNPs/GP) sample.

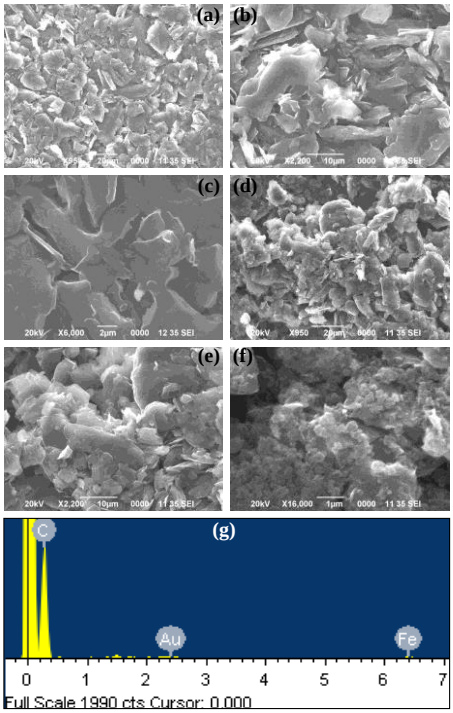

Fig. 1 SEM images for (a-c) graphite paste and (d-f) FePc-AuNPs modified graphite paste samples. (g) EDX profile for FePc-AuNPs/GP, confirming the presence of Au and Fe in the graphite paste.

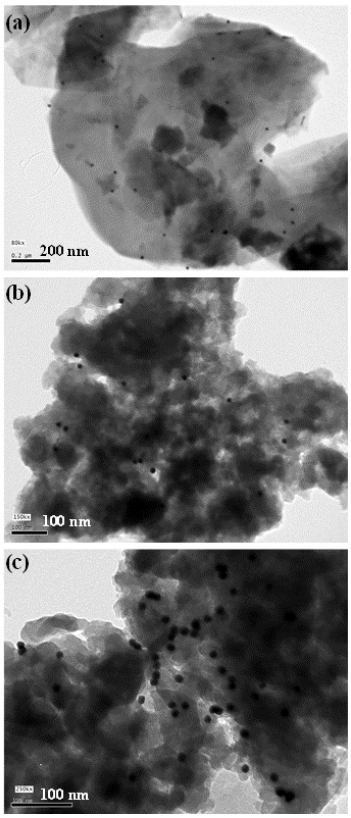

Fig. 2 TEM images (a-b) FePc-AuNPs/G and (c) FePc-AuNPs samples.

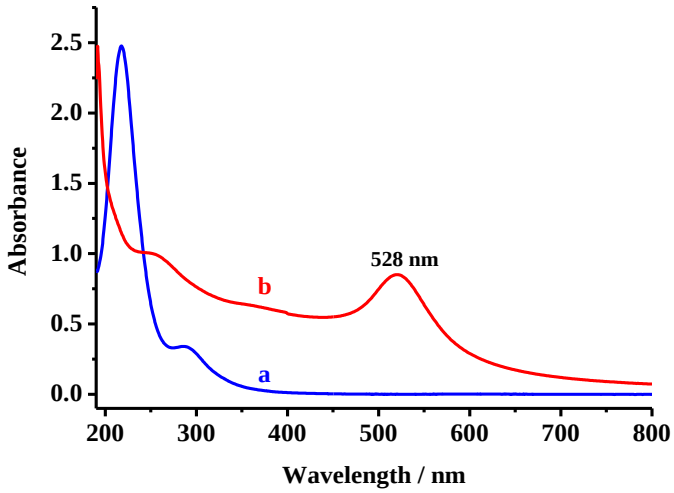

Fig. 3 UV-visible spectra for (a) Au precursor salt and (b) Au nanoparticles.

The particle size and distribution for Au nanoparticles were confirmed by TEM analysis. The prepared suspensions were subjected to vigorous sonication prior to measurements. The TEM images for FePc-AuNPs and FePc-AuNPs/G samples are shown in Fig. 2. From the comparison of TEM images over the same magnification, the presence of AuNPs is quite clear, while FePc exhibits carbon like morphology (dark clouds, likewise carbon). From the TEM analysis, it was observed that to some extent Au nanoparticles are well dispersed within a narrow particle-size distribution which is an indication of the homogenous carbon paste formation and particle dispersion. The dispersion of nanoparticles is crucial for a uniform paste formation and to avoid any particle agglomeration. The average particle size for Au nanoparticles was found to be 13±2nm. Overall, SEM/EDX and TEM studies confirm the particle size/dispersion, elemental confirmation and homogeneous morphology for the AuNPs-FePc incorporated graphite paste sample. In addition, the presence of Au nanoparticles was also confirmed via UV-visible spectroscopy. Fig. 3 shows the spectra for the gold precursor salt solution and gold nanoparticles with characteristic absorption peak at 528 nm confirming successful formation of Au nanoparticles.

3.2 Electrochemical characterizations

The graphite paste electrodes were characterised using cyclic voltammetry by potential scanning in 5 mM $[Fe(CN)_6]^{3-/4-}$ solution in 0.1 M KCl over the potential window 0.7 V to -0.4 V at a scan rate 0.1 V/s. The graphite paste electrode (Fig. 4a, electrode labelled 1 in Table 1) shows an oxidation and reduction peaks that are related to the electron transfer process (ΔE_p = 448 mV) between the electrode and $[Fe(CN)_6]^{3-/4-}$ solution. The oxidation and reduction peak currents of the GP electrode has been significantly enhanced by the addition of AuNPs to the paste with an oxidation peak at more negative potential and a reduction peak at more positive potential (ΔE_p = 321 mV) compared to that of the GP electrode. This demonstrates (Fig. 4b, electrode labelled 9 in Table 1) the role of AuNPs and associated high conductivity and characteristics of the Au nanoparticles. Furthermore, the electron transfer process has benefited from the addition of FePc to the graphite paste (Fig. 4c, ΔE_p = 297 mV for FePc-GP, electrode labelled 4 in Table 1) and by the addition of AuNPs to the FePc modified

graphite paste (Fig. 4d, ΔE_p = 219 mV for FePc-AuNPs/GP, electrode labelled 7 in Table 1). This is quite clear and well confirmed by the ease of oxidation and reduction (redox couple oxidised at more negative potential and reduced at more positive potential). The inclusion of AuNPs resulted in the improved electron transfer process of the graphite paste. The FePc-modified electrode showed improved electron transfer response compared to the blank/unmodified graphite paste electrode, which is attributed to the presence of FePc mediator. Overall, the inclusion of both AuNPs and FePc into the graphite paste (FePc-AuNPs/GP) resulted in improvement in the electron transfer characteristics. The enhanced response for FePc-AuNPs/GP electrode could be attributed to the properties of the Au nanoparticles and catalytic potential of the FePc catalyst. It is well known that dispersed Au nanoparticles are capable of improving the catalytical activity in bimetallic systems. This improvement is further discussed in the EIS studies. The peak at -0.2 V is attributed to $Fe^{II}Pc/Fe^{III}Pc$.

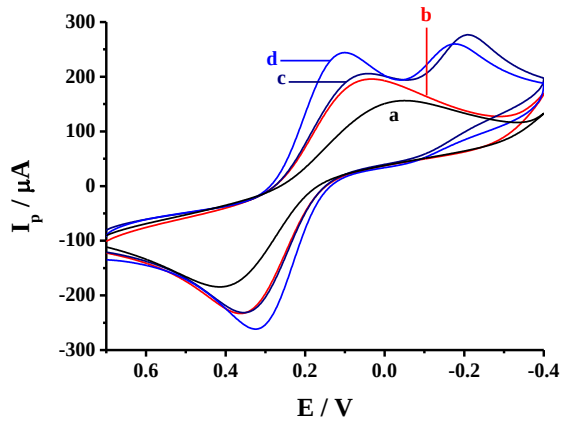

Fig. 4 Cyclic voltammograms of (a) GP, (b) AuNPs/GP, (c) FePc-GP and (d) FePc-AuNPs/GP electrodes in 5mM $[Fe(CN)_6]^{3-/4-}$ in 0.1M KCl solution.

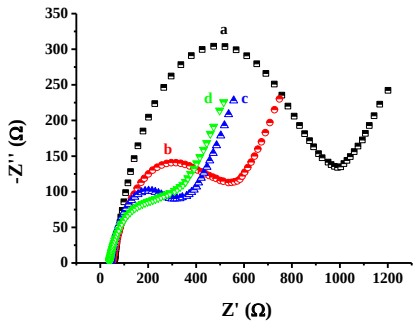

Fig. 5 EIS for different electrodes; (a) GP, (b) AuNPs/GP, (c) FePc-GP and (d) FePc-AuNPs/GP electrodes in 5mM $[Fe(CN)_6]^{3-/4-}$ solution (initial potential 0.22V, frequency range 0.1 Hz to 10^5 Hz).

Table 1 Compositions of different electrodes and R_{ct} values.

Electrode	Graphite (mg)	FePc (mg)	Paraffin (mg)	AuNPs[1] (%)	R_{ct} (Ω)
1	180.0	-	90	-	690.7
2	178.2	2.7 (1%)	89.1	-	368.7
3	174.6	8.1 (3%)	87.3	-	267.9
4	171.0	13.5 (5%)	85.5	-	207.2
5	167.4	18.9 (7%)	83.7	-	255.1
6	[2]171.0	13.5 (5%)	85.5	0.02%	155.4
7	[2]171.0	13.5 (5%)	85.5	0.055%	146.5
8	[2]171.0	13.5 (5%)	85.5	0.11%	167.5
9	[2]180.0		90	0.055%	310.8

[1] Percent of AuNPs in the paste. AuNPs stock solution was 58 mg/L.
[2] Milligrams of AuNPs/graphite composite used.

EIS is an effective tool for studying the interfacial properties of the surface-modified electrodes. The complex impedance was displayed as the sum of the real and imaginary components (Z_{re} and Z_{im}). By using the $[Fe(CN)_6]^{3-/4-}$ redox couple as the electrochemical probe, Nyquist plots for different graphite paste electrodes were investigated in the frequency range from 0.1 Hz to 10^5 Hz at 0.22 V as shown in Fig. 5. The typical impedance spectra include a semicircle portion at higher frequencies corresponding to the electron transfer-limited process and a linear part at the lower frequency range representing the diffusion limited process. The semicircle diameter in the impedance spectrum is a measure of the charge transfer-resistance (R_{ct}). This resistance controls the electron-transfer kinetics of the redox couple at the electrode interface. Therefore, R_{ct} can be used to describe the interfacial properties of the electrode. The unmodified paste electrode (GPE) shows a significant resistance to the electron transfer process as shown in Fig. 5a, it has a large semicircle domain (R_{ct} = 690 Ω). The inclusion of AuNPs within the paste composition showed an expected decrease in the resistance (Fig. 5b, R_{ct} = 310.8 Ω). The addition of FePc modifier (5%, Fig 5c) to the graphite paste shows a smaller semicircle domain (R_{ct} = 207 Ω) implying a lower electron-transfer resistance of the redox couple, which is due to the presence of the redox mediator iron phthalocyanine. Further the addition of AuNPs to the FePc modified graphite paste (FePc-AuNPs/GP, 0.055%, Fig. 5d), greatly decreased R_{ct} value to 146.5 Ω showing the influence of AuNPs on the electron transfer process.

Furthermore, various concentrations of FePc and AuNPs were investigated with the view to further improve the graphite paste characteristics. The percentage of FePc modifier was determined and optimised according to EIS studies. As is clear from the Fig. 6A and Table 1, by increasing the FePc modifier percentage, the resistance of the paste (R_{ct}) decreases until 5% FePc modifier ((from 1% to 5%, electrodes labelled 2-4 in Table 1), due to the catalytic activity of FePc. Any further increment in FePc percentage resulted in resistance increment (7%, electrode labelled as 5, Table 1) may be due to the reason that paste became hindered with the modifier and may impede the transfer process. Therefore we optimised 5% FePc modifier for further investigations as it showed the best performance characteristics.

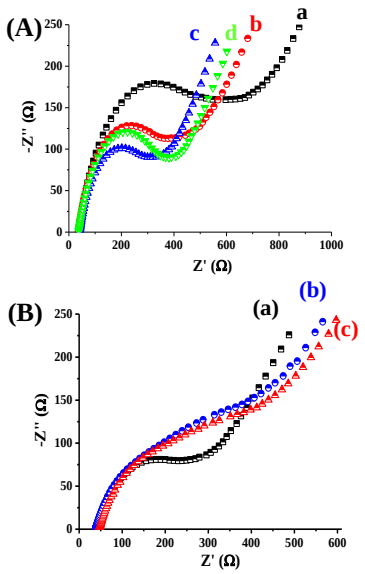

Fig. 6 (A) EIS response comparison among different FePc concentrations in the paste; (a) 1%, (b) 3%, (c) 5% and (d) 7%. (B) EIS response for AuNPs concentration variations with 5% FePc; (a) 0.02%, (b) 0.055% and (c) 0.11%. EIS parameters for both the experiments; initial potential 0.22 V (0.1 Hz to 10^5 Hz) in 5 mM $[Fe(CN)_6]^{3-/4-}$ solution.

Three electrodes with fixed FePc content (5%) but using different AuNPs percentages (electrodes labelled 6-8 in Table 1) were fabricated and investigated as shown in Fig. 6B and Table 1. The electrode labelled as 7 (Table 1), contains 0.055% of AuNPs and 5% FePc possesses lower resistance compared to electrode 6 (0.02% AuNPs and 5% FePc). This confirms that the resistance decreases by increasing the amount of AuNPs in the paste. Any further increase in AuNPs was not accompanied by any significant decrease in the electron transfer resistance (R_{ct}), possibly due to the agglomeration of Au nanoparticles with increasing Au content in the paste. Thus, the electrode labelled as 7, seems the most relevant option for further studies. From all the investigations (Fig 6 and Table 1), the electrode (labelled as 7 in Table 1) that contains 0.055% AuNPs and 5% FePc was optimised and proposed as a voltammetric sensor for cysteine due to the presence of Au nanoparticles and FePc redox mediator which collectively facilitate the oxidation of cysteine. The compositions of different stages of electrode modifications and its R_{ct} values are summarised in Table 1.

4. Electro-analytical Studies

4.1 Electrochemical determination of cysteine.

The modified and bare graphite paste electrodes were examined in relation to cysteine response. Fig. 7 shows the cyclic voltammetry response for (a) graphite paste (GP), (b) AuNPs/GP, (c) FePc-GP and (d) FePc-AuNPs/GP electrodes in the presence of cysteine (1 mM) in 0.1 M PBS solution (pH 7.4) over the potential window (0.0 V to 1.0 V) at a scan rate of 0.1 V/s. The AuNPs/GP (Fig. 7b) and FePc-GP (Fig. 7c) modified electrodes showed improved performance characteristics compared to GP electrode (Fig. 7a) under similar experimental conditions, and resulted in enhancement of the cysteine oxidation current.

Another striking characteristic feature is an obvious oxidation peak to cysteine at 0.75 V due to the presence of redox mediator, iron phthalocyanine, which highly facilitated the electrochemical oxidation of cysteine.

The AuNPs-FePc modified paste electrode (Fig. 7d) further showed improved characteristic features in the presence of cysteine. FePc-AuNPs/GPE oxidises cysteine at 0.62 V and demonstrated the role of AuNPs in the graphite paste to improve the performance. The cathodic shift of 130 mV in the presence of cysteine, is quite significant and demonstrates the importance of AuNPs in improving the paste and electrode characteristics. The sulfhydryl group of cysteine has a pK_a ~ 8.4 and it is reported that at pH 7.4, about 10% of free cysteine sulfhydryl groups are deprotonated and therefore negatively charged and ~ 90% were protonated.[27] The suggested mechanism for the oxidation of cysteine is based on the formation of extra coordinated complex between the cysteine sulfhydryl group and the metal centre of the phthalocyanine molecule followed by electron transfer and oxidation of cysteine to cystine.[28]

$$\text{Fe (III) Pc}^+ + \text{RSH} \rightarrow [\text{Fe (III) Pc-RS}] + \text{H}^+$$

$$[\text{Fe (III) Pc-RS}] \rightarrow \text{Fe (III) Pc}^+ + \text{RS}\bullet + \text{e}^-$$

$$2\text{RS}\bullet \rightarrow \text{RSSR}$$

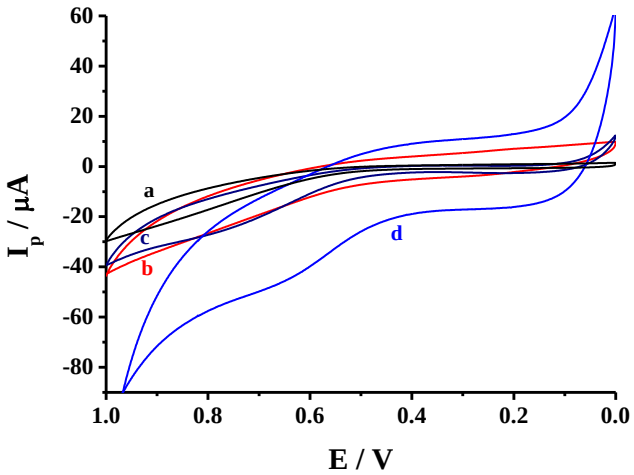

Fig. 7 Cyclic voltammograms of (a) GP, (b) AuNPs/GP, (c) FePc-GP and (d) FePc-AuNPs/GP electrodes in 1mM cysteine in 0.1M PBS solution (pH 7.4).

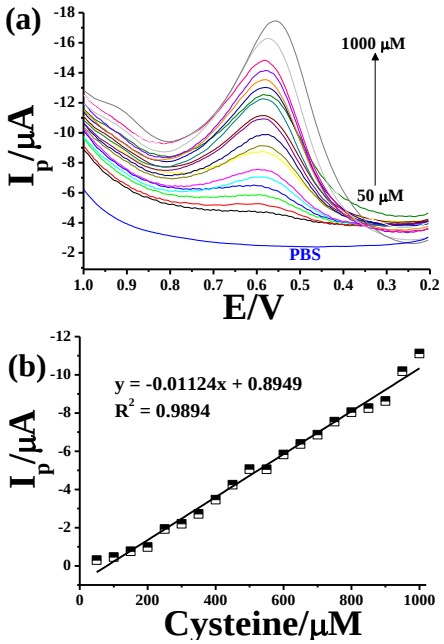

Fig. 8 (a) Differential pulse voltammetry response for AuNPs-FePc-GP at different concentrations (50-1000 µM) of cysteine in 0.1M PBS (pH 7.4) at potential 0.55 V. (b) Calibration curve for FePc-AuNPs/GP response over the different concentrations of cysteine.

A calibration curve (Fig. 8) for optimised FePc-AuNPs/GP electrode towards different cysteine concentrations was obtained using differential pulse voltammetry at the physiological pH (7.4), over the potential range 0.2 V to 1.0 V. For differential pulse voltammetry measurements, the following parameters were applied; Incr E = 0.004 V, Amplitude = 0.05 V, Pulse-width = 0.05 s, Sample-width = 0.0167 s, Pulse-period = 0.5 s. The cysteine oxidation current for the FePc-AuNPs/GPE was plotted against cysteine concentrations and the relationship showed a good linearity with R^2= 0.9894. The calibration curve shows the sensitivity value which is 11.24 µA/mM (57.2 µA/mM cm^2) and the linear range is from 50 µM to 1mM with a limit of detection of 0.27 µM.

(Table 2)

The repeatability (intra-electrode) of the current response has been tested for the optimised electrode (FePc-AuNPs/GP) by measuring 5 fresh solutions of 200 µM cysteine in PBS with % *RSD* of 7.2%. In addition, the reproducibility (inter-electrode) of 5 fresh electrodes with the same optimised compositions has been tested at the same concentration (200 µM cysteine) and the calculated % *RSD* value was 9.6%. This further demonstrated the capability of the proposed electrode (FePc-AuNPs/GP). Table 2 summarises a comparison of similar reports in the literature providing evidence of the analytical benefits obtained via the use FeMAPc and AuNPs in the paste composition for cysteine detection. It also shows that this work possess a wide linear range and a good limit of detection when compared with prior reports.

4.2 Interference and real application studies

Possible interferences which may occur in the practical determination of cysteine were investigated at the FePc-AuNPs/GP electrode. In the case of biomedical applications the average blood concentration of glutathione and methionine is in the range from 5-10 µM, while that of L-cysteine is from 230-260 µM.[38,39]

Table 3 Interference response data for FePc-AuNPs/GP.

Interferent	Recovery %		
	1:1	1:2	1:3
Glutathione	91.7	99.8	92.6
Methionine	88	85	92.6
Ascorbic acid	57.6	45	31.6
Ascorbic acid + Heat	96	87	85.4

Table 4 Determination of L-cysteine in pharmaceutical sachets and a dietary supplement using FePc-AuNPs/GP.

Sample	Added (ppm)	Found (ppm)	Recovery (%)
ACC sachets	74.23	74.50	100.4 (±2.6)
Glutathione enhancer	80.96	80.43	99.35 (±3.7)

Ascorbic acid (vitamin C) concentrations in plasma is tightly controlled and is about 80-90 µM,[40] irrespective of the daily dose. It is obvious that the concentration of the possible interferent in an important matrix like blood plasma is relatively low. The percentage change in the current response of cysteine is measured by addition of up to 3-folds of glutathione, methionine and ascorbic acid to a certain concentration of cysteine. The influence of these interferences on cysteine determination is measured as a percent recovery from the original current of cysteine prior to addition of interferents. Table 3 represents the interference studies for different ratios of the interferents relative to cysteine. By increasing the ratio of glutathione and methionine to cysteine, a small decrease was observed in the original current value of cysteine. Ascorbic acid showed a high interference reached to 68.4% at 3-folds of ascorbic acid.

The proposed electrode (FePc-AuNPs/GP) was employed in the analysis of measured acetyl cysteine (ACC) in pharmaceutical sachets (Acetylcistein, SEDICO Co.) (Table 4). Each sachet (4.7 g) contains 200 mg ACC. 47 mg of the sachet (2 mg ACC) was dissolved in 20 mL of PBS (pH 7.4). 100 ppm of ACC sachet was measured as cysteine (74.2 ppm) using the FePc-AuNPs/GP electrode (n=3). Another sample was a dietary supplement (Glutathione enhancer, Marcyrl Co.), where each capsule has 250 mg vitamin C, 100 mg N-acetyl cysteine, 50 mg glutathione, 50 mg L-cysteine, 50 mg L-methionine and 10 µg selenium. The capsule contents were dissolved in 100 mL of 0.1 M PBS (pH 7.4) and then 1.3 mL of this solution was diluted to 20 mL with PBS. The obtained signal was for both L-cysteine and N-acetyl cysteine. The sample was heated at 50°C for 30 min. to eliminate the interfering action of Vitamin C.

5. Conclusions

Gold nanoparticles and iron(III) phthalocyanine modified carbon paste based electrochemical sensor was designed and investigated for sensitive and selective cysteine determination in neutral pH conditions. The sensor was characterised using microscopic and electrochemical techniques. The inclusion of AuNPs into the carbon paste based samples, greatly decreased electron transfer resistance and revealed improved electron transfer characteristics due to its synergetic effect on the FePc

modified paste. The carbon paste sensor with AuNPs (0.055%) and FePc (5%), showed the optimum sensitivity for cysteine determination using DPV over the range 50-1000 μM, with LOD of 0.27 μM. The sensor showed a selective response in the presence of common interferences and its real potential was investigated in the determination of cysteine in some pharmaceutical preparations.

Acknowledgements

Authors thank the EU for supporting this work through FP7 Marie Curie IRSES **Project:** Micro/nano sensors for early cancer warning system – diagnostic and prognostic information "SMARTCANCERSENS".

[a] Electroanal. Lab., Applied Organic Chemistry Department, National Research Centre, Dokki, Cairo, Egypt. E-mail: dr.nooreldin@yahoo.com; Tel: +201001530137.

[b] Centre for Research in Electroanalytical Technologies (CREATE), Institute of Technology Tallaght (ITT Dublin), Dublin 24, Ireland.

Table 2 Comparison of this work with prior reports of cysteine detection.

Electrode material	Technique	*LR* (μM)	*LOD* (μM)	Ref.
[1]CuHCF/GE	CV, chronoamperometry	1-13	0.13	29
CuHCF/CPE	LSV	120-830	0.63	30
[2]Fe_2O_3@CoHCF	CV, chronoamperometry	5-37	0.48	31
Fe_2O_3@CoHCF	LSV	12.2-66.7	0.205	32
[3]PDMA/FMCPE	Chronoamperometry	80-2250	61.7	33
Co(II) salophen/CPE	DPV chronoamperometry	3-770	0.5	34
Co(II)-4-methylsalophen/CPE	CV, DPV	0.5-100	0.2	35
DTNB/GNPs/PEI/MWCNTs/GCE	Chronoamperometry	9-250	2.7	36
Oxovanadium(IV) salen/CPE	Chronoamperometry	240–2300	170	37
FePc-AuNPs/GPE	DPV	50-1000	0.27	This work

[1] Copper hexacyanoferrate/graphite electrode

[2] Iron(III) oxide core–cobalt hexacyanoferrate shell

[3] poly N,N-dimethylaniline/ferrocyanide film modified carbon paste electrode

References

1 X. Chen, S.-K. Ko, M. J. Kim, I. Shin, J. Yoon, *Chem. Commun.*, 2010, **46**, 2751–2753.
2 L. Yonge, S. Gracheva, S. J. Wilkins, C. Livingstone, J. Davis, *J. Am. Chem. Soc.*, 2004, **126**, 7732–7733.
3 W. H. Wang, O. Rusin, X. Y. Xu, K. K. Kim, J. O. Escobedo, S. O. Fakayode, K. A. Fletcher, M. Lowry, C. M. Schowalter, C. M. Lawrence, F. R. Fronczek, I. M. Warner, R. M. Strongin, *J. Am. Chem. Soc.*, 2005, **127**, 15949–15958.
4 Y. Hsiao, W. Su, J. Cheng, S. Cheng, *Electrochimica Acta*, 2011, **56**, 6887–6895.
5 Z. M. Liu, J. H. Li, S. J. Dong, E. K. Wang, *Anal. Chem.*, 1996, **68**, 2432–2436.
6 J. V. Ros-Lis, B. Garcia, D. Jiménez, R. Martinez-Manez, F. Sancenon, J. Soto, F. Gonzalvo, M. C. Valldecabres, *J. Am. Chem. Soc.*, 2004, **126**, 4064–4065.
7 Y. Wang, J. Lu, L. H. Tang, H. X. Chang, J. H. Li, *Anal. Chem.*, 2009, **81**, 9710–9715.
8 N. Spataru, B. V. Sarada, E. Popa, D. A. Tryk, A. Fujishima, *Anal. Chem.*, 2001, **73**, 514–519.
9 J. A. Reynaud, B. Maltoy, P. J. Canessan, *Electroanal. Chem.*, 1980, **114**, 195–211.
10 M. E. Johll, D. G. Williams, D. C. Johnson, *Electroanalysis*, 1997, **9**, 1397–1402.
11 C. Terashima, T. N. Rao, B. V. Sarada, Y. Kubota, A. Fujishima, *Anal. Chem.*, 2003, **75**, 1564–1572.
12 M. Ahmad, C. F. Pan, J. J. Zhu, *J. Mater. Chem.*, 2010, **20**, 7169–7174.
13 J. M. Zen, A. S. Kumar, J. C. Chen, *Anal. Chem.*, 2001, **73**, 1169–1175.
14 T. Inoue, J. R. Kirchhoff, *Anal. Chem.*, 2000, **72**, 5755–5760.
15 Y.-Q. Zhang, Y.-J. Fan, L. Cheng, L.-L. Fan, Z.-Y. Wang, J.-P. Zhong, L.-N. Wu, X.-C. Shen, Z.-J. Shi, *Electrochim. Acta*, 2013, **104**, 178–184.
16 C. G. Claessens, U. Hahn, T. Torres, *The Chemical Record*, 2008, **8**, 75-97.
17 J.-S. Ye, Y. Wen, W. D. Zhang, H. F. Cui, G. Q. Xu, F.-S. Sheu, *Electroanalysis*, 2005, **17**, 89-96.
18 P. Mashazi, T. Mugadza, N. Sosibo, P. Mdluli, S. Vilakazi, T. Nyokong, *Talanta*, 2011, **85**, 2202-2211.
19 C. W. Foster, J. Pillay, J. P. Metters, C. E. Banks, *Sensor*, 2014, **14**, 21905-21922.
20 K. I. Ozoemena, J. Pillay, T. Nyokong, *Electrochem. Comm.*, 2006, **8**, 1391–1396.
21 J. Pillay, K. I. Ozoemena, *Electrochim. Acta*, 2009, **54**, 5053-5059.
22 F. C. Moraes, L. H. Mascaro, S. A. S. Machado, C. M. A. Brett, *Electroanalysis*, 2010, **22**, 1586-1591.
23 S. Pakapongpan, J. P. Mensing, D. Phokharatkul, T. Lomas, A. Tuantranont, *Electrochim. Acta*, 2014, **133**, 294–301.
24 J. Metz, O. Schneider, M. Hanack, *Inorg. Chem.*, 1984, **23**, 1065-1071.
25 D. Aili, K. Enander, J. Rydberg, I. Nesterenko, F. Bjorefors, L. Baltzer, B. Liedberg, *J. Am. Chem. Soc.*, 2008, **130**, 5780-5788.
26 K. M. de Oliveira, T. C. C. dos Santos, L. R. Dinelli, J. Z. Marinho, R. C. Lima, A. L. Bogado, *Polyhedron*, 2013, **50**, 410-417.
27 A. Nezamzadeh-Ejhieh, H. Hashemi, *Talanta*, 2012, **88**, 201–208.
28 L. G. Shaidarova, S. A. Ziganshina, A. V. Gedmina, I. A. Chelnokova, and G. K. Budnikov, *Journal of Analytical Chemistry*, 2011, **66**, 633–641.
29 M. R. Majidi, K. Asadpour-Zeynali, B. Hafezi, *Microchim. Acta*, 2010, **169**, 283-288.
30 W. T. Suarez, L. H. Marcolino, O. Fatibello-Filho, *Microchem. J.*, 2006, **82**, 163‑167.
31 N. Sattarahmady, H. Heli, *Anal. Biochem.*, 2011, **409**, 74-80.
32 H. Heli, S. Majdi, N. Sattarahmady, *Sensors and Actuators B*, 2010, **145**, 185–193.
33 R. Ojani, J. B. Raoof, E. Zarei, *J. Electroanal. Chem.*, 2010, **638**, 241-245.
34 M. K. Amini, J. H. Khorasani, S. S. Khaloo, S. Tangestaninejad, *Anal. Biochem.*, 2003, **320**, 32‑38.
35 S. Shahrokhian, M. Karimi, *Electrochim. Acta*, 2004, **50**, 77‑84.
36 M. Santhiago, P. R. Lima, W. J. R. Santos, L. T. Kubota, *Sensors and Actuators B*, 2010, **146**, 213-220.
37 M. F. S. Teixeira, E. R. Dockal, E. T. G. Cavalheiro, *Sensors and Actuators B*, 2005, **106**, 619-625.
38 J. S. Chung, R. Haque, D.N. G. Mazumder, L. E. Moore, N. Ghosh, S. Samanta, S. Mitra, M. M. Hira-Smith, O. von Ehrenstein, A. Basu, J. Liaw, A. H. Smith, *Environmental Research* , 2006, **101**, 230–237.
39 A. Pastore, F. Piemonte, M. Locatelli, A. Lo Russo, L. Maria Gaeta, G. Tozzi, G. Federici *Clinical Chemistry*, 2001, **47**, 1467-1469.

40 M. Levine, S. J. Padayatty, M. G. Espey, *American Society for Nutrition. Adv. Nutr*. 2011, **2**, 78–88.